Controlling Terahertz Radiation with Nanoscale Metal Barriers Embedded in Nano Slot Antennas

Hyeong-Ryeol Park,[†] Young-Mi Bahk,[†] Kwang Jun Ahn,[†] Q-Han Park,[‡] Dai-Sik Kim,[†,*] Luis Martín-Moreno,[§] Francisco J. García-Vidal,[⊥,*] and Jorge Bravo-Abad[⊥]

[†]Center for Subwavelength Optics, Department of Physics and Astronomy, Seoul National University, Seoul 151-747, Korea, [‡]Department of Physics, Korea University, Seoul 136-701, Korea, [§]Instituto de Ciencia de Materiales de Aragón and Departamento de Física de la Materia Condensada, CSIC—Universidad de Zaragoza, E-50009 Zaragoza, Spain, and [⊥]Departamento de Física Teórica de la Materia Condensada, Universidad Autónoma de Madrid, E-28049 Madrid, Spain

ABSTRACT Nanoscale metallic barriers embedded in terahertz (THz) slot antennas are shown to provide unprecedented control of the transition state arising at the crossover between the full- and half-wavelength resonant modes of such antennas. We demonstrate strong near-field coupling between two paired THz slot antennas separated by a 5 nm wide nanobarrier, almost fully inducing the shift to the resonance of the double-length slot antenna. This increases by a factor of 50 the length-scale needed to observe similar coupling strengths in conventional air-gap antennas (around 0.1 nm), making the transition state readily accessible to experiment. Our measurements are in good agreement with a quantitative theoretical modeling, which also provides a simple physical picture of our observations.

KEYWORDS: terahertz spectroscopy · terahertz nano slot antenna · subskin depth barrier · nanoparticle detection · paired antenna

Optical antennas are perhaps one of the most versatile concepts in nano-optics. Their unique ability to manipulate and control electromagnetic (EM) fields at the subwavelength scale makes optical antennas excellent candidates for enhancing the performance of a vast variety of applications, including photodetection, photovoltaics, enhanced nonlinear optics, and biological imaging.[1,2] One of the most common realizations of optical antennas consists of a simple metallic nanostructure formed by two similar elements (such as nanoshells,[3] nanorods,[4] or nanoparticles[5−7]) separated by an air or dielectric nanogap (see a schematic illustration in Figure 1a, left). These *positive* nanoantennas have already demonstrated subwavelength field enhancement,[8] nanoparticle detection,[9] and pattern-tuning ability[10,11] in the visible and infrared frequency regimes. Within this general endeavor, one important topic that has not yet been fully explored is the continuous transition from the half- to the full-wavelength resonance that occurs when the nanogap between the two adjacent metallic elements forming the antenna is decreased up to where these two elements merge completely (see schematics in top panel of Figure 1b). Despite the vast potential of this kind of analysis for exploring fundamental physics as well as to enable unique device applications, the observation of that transition state has not yet been reported. This is due to the severe technical challenges it poses, such as the fabrication of subnanometer air gaps with an accuracy of less than 0.1 nm.[12−14]

On the other hand, when we consider two paired "negative" slot antennas (see schematics of the proposed structure in Figure 1a, right) with a metallic nanoscale barrier, slots replacing metals and the metallic barrier replacing the air gap, another important length scale enters. The coupling between the paired slots changes drastically as the barrier width decreases from the skin depth (δ) to extreme subskin depth (see a schematics of this evolution in Figure 1b, bottom). In this sense, Babinet's principle[15] is not applicable when comparing antennas and slot antennas with subskin depth barriers. This is because the strongly enhanced resonant electric field inside each slot can penetrate through the subskin depth barrier, to couple the adjacent resonant modes, and generate a new resonant mode. For positive antennas, the gap still needs to be on the order of 1 nm or less to see strong coupling. The deep subskin depth regime, despite its vast potential for exploring fundamental physics and for unique device applications, has not been fully explored.

In this article, we report on a novel approach to observe the continuous evolution between the full- and half-wavelength

* Address correspondence to dsk@phya.snu.ac.kr, fj.garcia@uam.es.

Received for review August 19, 2011 and accepted September 30, 2011.

Published online September 30, 2011
10.1021/nn2031885

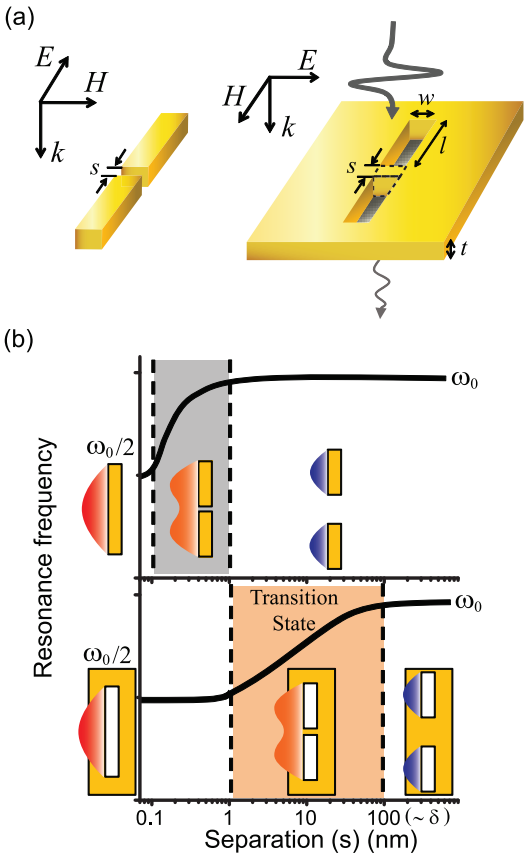

Figure 1. (a) Schematics of (left) a paired positive antennas with an air nano gap of width *s* and (right) a paired THz slot antennas separated by a metallic nanobarrier of a width *s*. In the slot antennas, the p-polarized lights with polarization perpendicular to the long axis of the rectangle are normally incident on the sample. (b) Comparison between (top) positive antennas and (bottom) negative slot antennas making resonance transitions from the resonance at frequency ω_0 of each individual antenna to the resonance at $\omega_0/2$ of the entire length antenna, depending on the separation between the two antennas.

resonant states supported by optical nanoantennas. By embedding a nanometric gold barrier in a terahertz (THz) slot antenna,[16−18] featuring a length of hundreds of micrometers but a nanoscale width, we create a *negative* paired antenna system in which the above-mentioned evolution occurs for barrier sizes readily accessible to experiment (Figure 1a, right). Specifically, by means of transmission measurements, we show that as the width of the metallic barrier is decreased from 100 nm (roughly the skin-depth δ of gold in the THz regime) to 5 nm ($\sim\delta/20$), the frequency of the resonance supported by the paired slot antenna continuously evolves from an original state at a frequency ω_0 to almost the $\omega_0/2$ resonance appearing in the double-length slot antenna (Figure 1b, bottom). Using a quantitative theoretical modeling based on a coupled-mode theory approach,[19] we provide a simple and intuitive picture that reveals the physical origin of these observations. Furthermore, we also provide experimental evidence on how the same concept can be

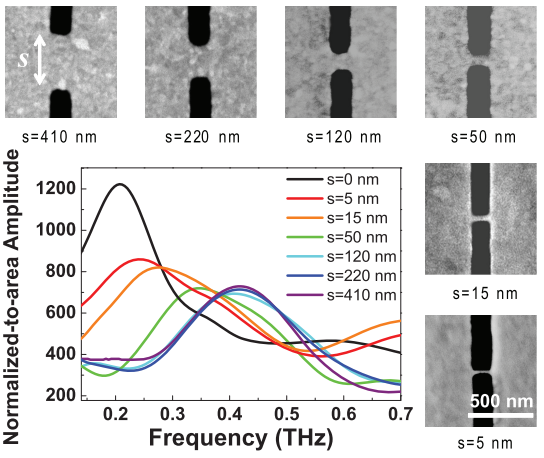

Figure 2. Experimental normalized-to-area amplitude spectra of two identical THz slot antennas (l = 150 μm and w = 120 nm) separated by various barriers of width s, surrounded by scanning electron microscopy (SEM) images of nanobarriers with s = 5, 15, 50, 120, 220, and 410 nm.

applied to detect a nanoparticle sitting on top of a slot antenna, which enables terahertz radiation to detect single nanoparticles.

RESULTS AND DISCUSSION

Figure 2 renders the normalized-to-area amplitude spectra as measured for six different nanobarriers, having mean widths (s) ranging from s = 5 to 410 nm, embedded in THz nano slot antennas with dimensions of a length l = 150 μm and a width w = 120 nm. For comparison, Figure 2 also includes the transmission spectrum corresponding to the slot antenna without nanobarrier (s = 0), as well as scanning electron microscopy (SEM) images of some of the considered nanobarriers. As observed in Figure 2, for values of s larger than 220 nm, the spectra are dominated by a peak appearing at 0.42 THz, which corresponds to the resonant frequency supported by each of the apertures separately.[16] The localization of this peak is a distinct manifestation of the negligible EM coupling existing between the two apertures for $s >$ 220 nm. As the width of the nanobarrier is decreased to values smaller than the skin-depth of gold (118 nm at 0.4 THz[20,21]), the location of the transmitted amplitude peak red shifts and its height increases. This yields transmission spectra that, as s decreases, start resembling that expected for an unperturbed slot antenna featuring a length of 2l. For the thinnest nanobarrier, we used, 5 nm wide which is already in the deep subskin depth regime, the resonance frequency occurs at 0.21 THz. This is already very close to the resonant frequency of a two-times-lengthened slot antenna, indicating strong coupling. To our knowledge, these results represent the first observation of the continuous transition from the half-wavelength to the full-wavelength states in a nanoscale metallic antenna.

To gain insight into the physical origin of this evolution of the transmission spectra, we use a theoretical formalism based on a modal expansion of the EM fields in the different regions of the structure. This framework can accurately deal with both the large aspect ratio displayed by the analyzed slot antennas (an aspect ratio of about 2500 is considered) as well as the vastly different length scale existing between the nanobarrier width and the long side of the metallic apertures forming the antenna. Notice that this combination of very different length scales limits the applicability to this problem of most of the standard numerical approaches often used in nano-optics, such as those based on the finite-difference time-domain (FDTD) method or three-dimensional finite-element discretization.

Within the applied theoretical formalism, the two-paired slot antennas and the metallic barrier separating them are considered as a single THz waveguiding structure. This waveguide can be viewed as a conventional rectangular metallic hollow waveguide perturbed by a nano-object placed in its interior. The first step of our theoretical analysis consists of computing, in the frequency range of interest, the dispersion relation and EM mode profiles of this special class of waveguide. Then, by extending to this problem the theoretical formalism described in ref 16, we calculate the EM fields in all space in terms of the modal amplitudes of the electric field at the illuminated and non-illuminated ends of the considered waveguide. The following two approximations were introduced when applying this theoretical approach. First, we consider perfect-metal boundary conditions in all *external* air−metal interfaces that are not in contact with the nanobarrier. For the metallic nanobarrier, we use a conventional Drude-like formula for its dielectric constant.[21] Second, we only consider the fundamental mode of the whole waveguide structure (formed by the two apertures and the metallic nanobarrier). The accuracy of both approximations was checked by comparing our predictions for small aspect ratio antennas with full numerical simulations performed with a commercial three-dimensional finite-element method (COMSOL Multiphysics) .

Figure 3a shows our numerical results for the normalized-to-area transmitted amplitude as computed for the seven different samples considered in Figure 2 and an additional one with $s = 1$ nm. As observed in this figure, there is a good quantitative agreement between the theoretical predictions and the corresponding experimental measurements displayed in Figure 2, both in the magnitude of the resonant peak and in the evolution with s of its line width and spectral location. The good agreement between the computed and measured resonant peak positions is more clearly visualized in Figure 3b. We emphasize that no fitting parameters are used in these calculations. The

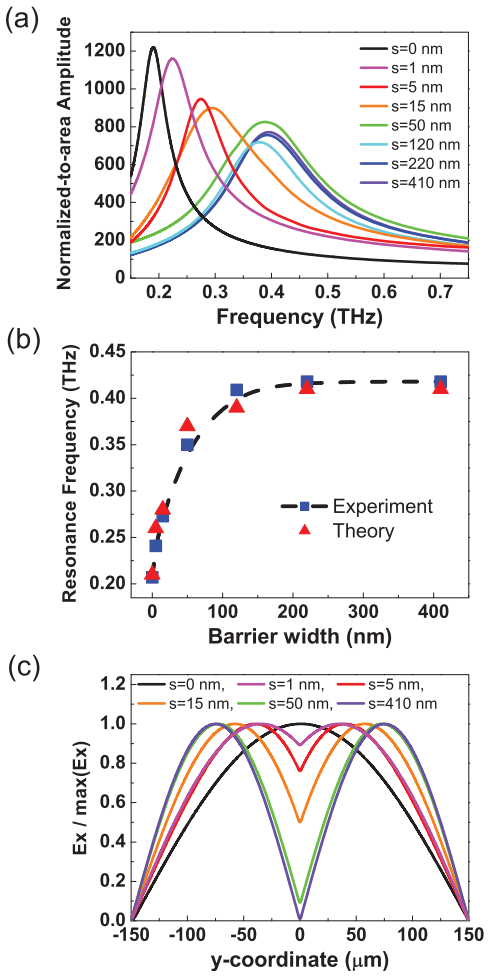

Figure 3. (a) Normalized-to-area amplitude computed for eight cases of the paired slot antennas with $l = 150$ μm and $w = 120$ nm considered in Figure 2. (b) Resonance frequencies of the paired slot antennas, depending on the width of nanobarrier. (c) Simulated electric field profiles corresponding to the values of the nanobarrier width s shown in panel (a). For clarity, plots for $s = 120$ nm and $s = 220$ nm are not included in this panel.

discrepancies that arise when comparing theory and experiments can be attributed to the following three facts. First, although in our theory we have assumed the metallic barrier to be a perfectly rectangular block, SEM images of several transversal cross sections of the experimental samples show that the actual shape of the nanobarriers resembles a rectangular pyramid with rounded edges. We have observed that this difference between the theoretical and the actual shape of the nanobarrier is particularly evident for the thinnest barrier considered experimentally ($s = 5$ nm). Second, in our theory, we simulate the EM response of the nanobarrier by means of a Drude-like formula, using conventional bulk parameters for gold at THz frequencies.[21] However, it has been shown that those parameters can change in ultrathin metallic films.[22,23] This effect is again larger for the thinnest barriers considered in this work. Finally, another source of the discrepancy between the theoretical and experimental

results might arise from the change of the metallic properties of the system due to the presence of gallium introduced by the FIB milling process.[24] Despite these facts, we emphasize the remarkable good agreement found between theory and experiments, which definitely demonstrates the continuous transition from the ω_0 to the $\omega_0/2$ states as the barrier width is decreased.

Once the validity of our theoretical model has been checked by a direct comparison with the corresponding measurements, we turn now to provide an intuitive physical explanation of our observations. As in the case of a single rectangular hole perforated on a thick metallic film, the transmission peak can be attributed to the excitation of a *zero-order* Fabry–Perot resonance.[16] When dealing with subwavelength apertures, the phase accumulated by the EM field inside the aperture determines the resonance wavelength and has two sources. One is related to the optical path (*i.e.*, photon wavenumber times the thickness of the metal film), and the other is associated with the phase that the photon acquires when it impinges at the two interfaces of the aperture.[25] In our system, the slot antenna with an embedded nanobarrier is milled into an ultrathin metallic film ($t \ll \lambda$), and therefore, the formation of the resonance is mainly dictated by the reflection coefficient. This coefficient measures the coupling between the fundamental waveguide mode inside the aperture and the continuum of radiative modes existing at both the incidence and transmission regions (above and below the metallic film, respectively). Then, following this argument, the spectral location of the resonance of the whole system formed by the slot antenna and the nanobarrier will correspond to the wavelength when the total phase acquired upon reflection is zero (modulus 2π), which occurs when the coupling between the waveguide and the radiative modes is minimal.[26] In our discussion, the crucial point to realize is that the strength of the mentioned EM coupling with the radiation modes is governed by the in-plane electric-field profile $\mathbf{E}_t = (E_x,E_y)$ of the fundamental waveguide mode.[16,18] Thus, the spectral location of the EM resonance will only depend on the particular profile of $\mathbf{E}_t(\mathbf{r})$. This line of reasoning suggests that the physical origin of the evolution of the transmission spectra shown in Figures 2 and 3a relies on the modification that the presence of the nanobarrier induces in the near-field profile $\mathbf{E}_t(\mathbf{r})$ of the waveguide mode. In fact, on the basis of this analysis, and from the observed evolution of the spectra with *s*, we expect $\mathbf{E}_t(\mathbf{r})$ to evolve continuously from the *E*-field profile corresponding to the half-wavelength state to that of the full-wavelength state. In order to check this point, Figure 3c shows a series of *E*-field profiles as computed for the same values of *s* shown in Figures 2 and 3a. Only the E_x component is shown for each case since, for the considered incident polarization, it is the dominant component of the electric field

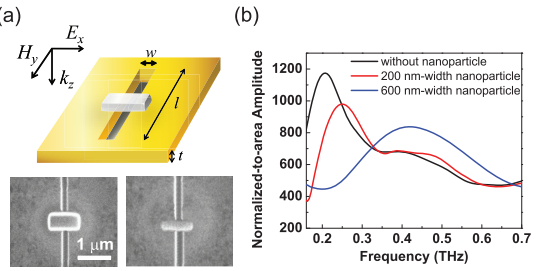

Figure 4. (a) Schematic of a Pt nanoparticle at the center position on the THz slot antenna with dimensions of a total length *l* = 300 μm and a width *w* = 120 nm. At the bottom, enlarged SEM pictures of the (left) larger and (right) smaller nanoparticles. (b) Normalized-to-area amplitude spectra of the THz slot antenna without nanoparticle, with the 600 nm width and 200 nm width nanoparticles at the center position.

within the structure. These results clearly show how, as the width of the nanobarrier is decreased, the EM coupling between the two resonances supported by each of the two subwavelength apertures forming the antennas starts merging and gives rise to a new mode. The numerics also show how the profile of this *transition state* converges to the *E*-field profile of the double-length antenna without nanobarriers, which accounts well for the corresponding convergence in the transmission spectra shown in Figures 2 and 3a.

Finally, to explore the significant potential application of these ideas for nanoparticle detection using terahertz radiation, we investigate whether a metallic nanoparticle placed on top of a slot antenna can shift the resonance, all the way to separating the two cavities. We introduce platinum (Pt) nanoparticles placed on the top of the THz slot antenna with dimensions of a total length *l* = 300 μm and a width *w* = 120 nm (Figure 4a). Pt nanoparticles are fabricated by a Pt deposition method using focused ion beam. The larger nanoparticle is 1 μm long, 600 nm wide, and has a thickness of 400 nm, while the smaller one has the same length, a width of 200 nm, and a thickness of 250 nm, so that the width and thickness are slightly smaller than the Pt skin depth of 280 nm at 0.4 THz. Figure 4b shows the normalized-to-area amplitude spectra, with the two nanoparticles at the center position, of the THz slot antenna with the fundamental resonance of 0.2 THz, as used in previous figures. The larger nanoparticle with 600 nm width at the midpoint turns off the fundamental and generates a new resonance twice larger than the fundamental resonance frequency. The 200 nm width nanoparticle affects the resonance much less, although a sizable shift is noticeable. Comparison with nanobarrier data indicates that the effective separation *s* introduced by a nanoparticle sitting on top of the aperture would be much smaller than its size, strongly suggesting that the resonance shift can be a very sensitive measure of the contact between the nanoparticle and the slot antenna.[27]

CONCLUSIONS

We have reported a novel route to access the continuous crossover between the half- and the full-wavelength states supported by an optical nanoantenna. The proposed system, consisting of a metallic nanobarrier embedded in a terahertz slot antenna, has enabled the observation of the transition state arising at this crossover. Our experimental findings are in good agreement with a numerical modeling of the EM response of the system, which also provides a simple physical explanation of our observations. The potential of this scheme has been further shown by extending our approach to the case of a metallic nanoparticle placed on top of a slot antenna. These results open new perspectives to tailor the flow of terahertz electromagnetic waves using deep subskin metallic nano-objects and may lead to the realization of novel schemes for ultrasensitive tuning and detection of nanoscale objects using electromagnetic radiation with a wavelength within the millimeter range.

METHODS

Experimental Method. To experimentally probe the antennas coupling across the subskin depth barriers, we measure the transmission spectra of THz slot antennas in the frequency range from 0.1 to 1.0 THz using THz time-domain spectroscopy.[28,29] The transmissivity through the samples is experimentally characterized by the normalized-to-area amplitude, equal to the average enhancement of the electric field inside the slot according to the vector Kirchhoff's formalism,[30,31] using a normalizing aperture of 3.4 mm $\times$ 2.5 mm dimensions.

Sample Fabrication. The THz slot antennas, patterned by focused ion beam, have dimensions of a length l = 150 μm and a width w = 120 nm in a gold film with thickness t = 60 nm deposited onto a 2 μm thick SiN/SiO_2 substrate (see right panel of Figure 1a for a sketch of the fabricated structure). To avoid the coupling between individual paired antennas, our samples consist of only four vertically aligned paired slot antennas with a vertical period of 310 μm.

Acknowledgment. This work was supported by the National Research Foundation of Korea (NRF) grant funded by the Korean government (MEST) (SRC, No. R11-2008-095-01000-0) (Nos. 2010-0029648, 2010-0028713, 2011-0019170), KICOS (GRL, K20815000003), and Hi Seoul Science/Humanities Fellowship from Seoul Scholarship Foundation, and by the Spanish Ministry of Science and Innovation under Project Nos. MAT2008-06609-C02, CSD2007-046-NanoLight.es, and by Grant No. RyC-2009-05489.

REFERENCES AND NOTES

1. Novotny, L.; van Hulst, N. Antennas for Light. *Nat. Photonics* **2011**, *5*, 83–90.
2. Giannini, V.; Fernandez-Dominguez, A. I.; Heck, S. C.; Maier, S. A. Plasmonic Nanoantennas: Fundamentals and Their Use in Controlling the Radiative Properties of Nanoemitters. *Chem. Rev.* **2011**, *111*, 3888–3912.
3. Prodan, E.; Radloff, C.; Halas, N. J.; Nordlander, P. A Hybridization Model for the Plasmon Response of Complex Nanostructures. *Science* **2003**, *302*, 419–422.
4. Muhlschlegel, P.; Eisler, H. J.; Martin, O. J. F.; Hecht, B.; Pohl, D. W. Resonant Optical Antennas. *Science* **2005**, *308*, 1607–1609.
5. Kim, Z. H.; Kim, D. S.; Heo, J.; Ahn, S. H.; Han, S. W.; Yun, W. S. Real-Space Mapping of the Strongly Coupled Plasmons of Nanoparticle Dimers. *Nano Lett.* **2009**, *9*, 3619–3625.
6. Atay, T.; Song, J. H.; Nurmikko, A. V. Strongly Interacting Plasmon Nanoparticle Pairs: From Dipole−Dipole Interaction to Conductively Coupled Regime. *Nano Lett.* **2004**, *4*, 1627–1631.
7. Fromm, D. P.; Sundaramurthy, A.; Schuck, P. J.; Kino, G.; Moerner, W. E. Gap-Dependent Optical Coupling of Single "Bowtie" Nanoantennas Resonant in the Visible. *Nano Lett.* **2004**, *4*, 957–961.
8. Schnell, M.; Garcia-Etxarri, A.; Alkorta, J.; Aizpurua, J.; Hillenbrand, R. Phase-Resolved Mapping of the Near-Field Vector and Polarization State in Nanoscale Antenna Gaps. *Nano Lett.* **2010**, *10*, 3524–3528.
9. Righini, M.; Ghenuche, P.; Cherukulappurath, S.; Myroshnychenko, V.; de Abajo, F. J. G.; Quidant, R. Nano-Optical Trapping of Rayleigh Particles and *Escherichia coli* Bacteria with Resonant Optical Antennas. *Nano Lett.* **2009**, *9*, 3387–3391.
10. Schnell, M.; Garcia-Etxarri, A.; Huber, A. J.; Crozier, K.; Aizpurua, J.; Hillenbrand, R. Controlling the Near-Field Oscillations of Loaded Plasmonic Nanoantennas. *Nat. Photonics* **2009**, *3*, 287–291.
11. Alu, A.; Engheta, N. Tuning the Scattering Response of Optical Nanoantennas with Nanocircuit Loads. *Nat. Photonics* **2008**, *2*, 307–310.
12. Lassiter, J. B.; Aizpurua, J.; Hernandez, L. I.; Brandl, D. W.; Romero, I.; Lal, S.; Hafner, J. H.; Nordlander, P.; Halas, N. J. Close Encounters between Two Nanoshells. *Nano Lett.* **2008**, *8*, 1212–1218.
13. Danckwerts, M.; Novotny, L. Optical Frequency Mixing at Coupled Gold Nanoparticles. *Phys. Rev. Lett.* **2007**, *98*, 026104.
14. Zuloaga, J.; Prodan, E.; Nordlander, P. Quantum Description of the Plasmon Resonances of a Nanoparticle Dimer. *Nano Lett.* **2009**, *9*, 887–891.
15. Ogut, B.; Vogelgesang, R.; Sigle, W.; Talebi, N.; Koch, C. T.; Aken, P. A. V. Hybridized Metal Slit Eigenmodes as an Illustration of Babinet's Principle. *ACS Nano* **2011**, *5*, 6701–6706.
16. Garcia-Vidal, F. J.; Moreno, E.; Porto, J. A.; Martin-Moreno, L. Transmission of Light through a Single Rectangular Hole. *Phys. Rev. Lett.* **2005**, *95*, 103901.
17. Park, H. R.; Park, Y. M.; Kim, H. S.; Kyoung, J. S.; Seo, M. A.; Park, D. J.; Ahn, Y. H.; Ahn, K. J.; Kim, D. S. Terahertz Nanoresonators: Giant Field Enhancement and Ultrabroadband Performance. *Appl. Phys. Lett.* **2010**, *96*, 121106.
18. Bahk, Y. M.; Park, H. R.; Ahn, K. J.; Kim, H. S.; Ahn, Y. H.; Kim, D. S.; Bravo-Abad, J.; Martin-Moreno, L.; Garcia-Vidal, F. J. Anomalous Band Formation in Arrays of Terahertz Nanoresonators. *Phys. Rev. Lett.* **2011**, *106*, 013902.
19. Garcia-Vidal, F. J.; Martin-Moreno, L.; Ebbesen, T. W.; Kuipers, L. Light Passing through Subwavelength Apertures. *Rev. Mod. Phys.* **2010**, *82*, 729–787.
20. Azad, A. K.; Zhang, W. L. Resonant Terahertz Transmission in Subwavelength Metallic Hole Arrays of Sub-Skin-Depth Thickness. *Opt. Lett.* **2005**, *30*, 2945–2947.
21. Ordal, M. A.; Long, L. L.; Bell, R. J.; Bell, S. E.; Bell, R. R.; Alexander, R. W.; Ward, C. A. Optical-Properties of the Metals Al, Co, Cu, Au, Fe, Pb, Ni, Pd, Pt, Ag, Ti, and W in the Infrared and Far Infrared. *Appl. Opt.* **1983**, *22*, 1099–1119.
22. Feng, B; Li, Z.; Zhang, X. Effect of Grain-Boundary Scattering on the Thermal Conductivity of Nanocrystalline Metallic Films. *J. Phys. D: Appl. Phys.* **2009**, *42*, 055311.
23. Liu, N.; Langguth, L.; Weiss, T.; Kastel, J.; Fleischhauer, M.; Pfau, T.; Giessen, H. Plasmonic Analogue of Electromagnetically Induced Transparency at the Drude Damping Limit. *Nat. Mater.* **2009**, *8*, 758–762.
24. Fu, Y.; Bryan, N. K. A. Investigation of Physical Properties of Quartz After Focused Ion Beam Bombardment. *Appl. Phys. B: Laser Opt.* **2005**, *80*, 581–585.

25. Garcia-Vidal, F. J.; Martin-Moreno, L. Transmission and Focusing of Light in One-Dimensional Periodically Nanostructured Metals. *Phys. Rev. B* **2002**, *66*, 155412–155421.
26. Rodrigo, S. G.; Carretero-Palacios, S.; Garcia-Vidal, F. J.; Martin-Moreno, L. To be published.
27. Park, H.; Park, J.; Lim, A. K. L.; Anderson, E. H.; Alivisatos, A. P.; McEuen, P. L. Nanomechanical Oscillations in a Single-C60 Transistor. *Nature* **2000**, *407*, 57–60.
28. Van exter, M.; Fattinger, C.; Grischkowsky, D. Terahertz Time-Domain Spectroscopy of Water-Vapor. *Opt. Lett.* **1989**, *14*, 1128–1130.
29. Wu, Q.; Litz, M.; Zhang, X. C. Broadband Detection Capability of ZnTe Electro-optic Field Detectors. *Appl. Phys. Lett.* **1996**, *68*, 2924–2926.
30. Kyoung, J. S.; Seo, M. A.; Park, H. R.; Ahn, K. J.; Kim, D. S. Far Field Detection of Terahertz Near Field Enhancement of Sub-wavelength Slits Using Kirchhoff Integral Formalism. *Opt. Commun.* **2010**, *283*, 4907–4010.
31. Seo, M. A.; *et al.* Terahertz Field Enhancement by a Metallic Nano Slit Operating beyond the Skin-Depth Limit. *Nat. Photonics* **2009**, *3*, 152–156.